JOURNAL OF PROTEOMICS 89 (2013) 95–111

Available online at www.sciencedirect.com

SciVerse ScienceDirect

www.elsevier.com/locate/jprot

Dracula's children: Molecular evolution of vampire bat venom

Dolyce H.W. Low[a,1], Kartik Sunagar[b,c,1], Eivind A.B. Undheim[a,d,1], Syed A. Ali[a,d,e,1], Alejandro C. Alagon[f], Tim Ruder[a], Timothy N.W. Jackson[a,d], Sandy Pineda Gonzalez[d], Glenn F. King[d], Alun Jones[d], Agostinho Antunes[b,c], Bryan G. Fry[a,d,*]

[a]Venom Evolution Lab, School of Biological Sciences, University of Queensland, St. Lucia, Queensland 4072, Australia
[b]CIMAR/CIIMAR, Centro Interdisciplinar de Investigação Marinha e Ambiental, Universidade do Porto, Rua dos Bragas, 177, 4050-123 Porto, Portugal
[c]Departamento de Biologia, Faculdade de Ciências, Universidade do Porto, Rua do Campo Alegre, 4169-007 Porto, Portugal
[d]Institute for Molecular Biosciences, University of Queensland, St. Lucia, Queensland 4072, Australia
[e]HEJ Research Institute of Chemistry, International Center for Chemical and Biological Sciences (ICCBS), University of Karachi, Karachi 75270, Pakistan
[f]Departamento de Medicina Molecular y Bioprocesos, Instituto de Biotecnología, Universidad Nacional Autónoma de México, Av. Universidad 2001, Cuernavaca, Morelos 62210, Mexico

ARTICLE INFO

Article history:
Received 29 March 2013
Accepted 28 May 2013

Keywords:
Molecular evolution
Vampire bat
Venom
Positive selection
Desmodus rotundus

ABSTRACT

While vampire bat oral secretions have been the subject of intense research, efforts have concentrated only on two components: DSPA (*Desmodus rotundus* salivary plasminogen activator) and Draculin. The molecular evolutionary history of DSPA has been elucidated, while conversely draculin has long been known from only a very small fragment and thus even the basic protein class was not even established. Despite the fact that vampire bat venom has a multitude of effects unaccounted by the documented bioactivities of DSPA and draculin, efforts have not been made to establish what other bioactive proteins are secreted by their submaxillary gland. In addition, it has remained unclear whether the anatomically distinct anterior and posterior lobes of the submaxillary gland are evolving on separate gene expression trajectories or if they remain under the shared genetic control. Using a combined proteomic and transcriptomic approach, we show that identical proteins are simultaneously expressed in both lobes. In addition to recovering the known structural classes of DSPA, we recovered a novel DSPA isoform as well as obtained a very large sequence stretch of draculin and thus established that it is a mutated version of the lactotransferrin scaffold. This study reveals a much more complex secretion profile than previously recognised. In addition to obtaining novel versions of scaffolds convergently recruited into other venoms (allergen-like, CRiSP, kallikrein, Kunitz, lysozyme), we also documented novel expression of small peptides related to calcitonin, PACAP, and statherin. Other overexpressed protein types included BPI-fold, lacritin, and secretoglobin. Further, we investigate the molecular evolution of various vampire bat venom-components and highlight the dominant role of positive selection in the evolution of these proteins. Conspicuously many of the proteins identified in the proteome were found to be homologous

* *Corresponding author at: Venom Evolution Lab, School of Biological Sciences, University of Queensland, St. Lucia, Queensland 4072, Australia.* Tel.: +61 400193182; fax: +61 733651692.
E-mail address: bgfry@uq.edu.au (B.G. Fry).
[1] Joint first authors.

http://dx.doi.org/10.1016/j.jprot.2013.05.034

to proteins with known activities affecting vasodilation and platelet aggregation. We show that vampire bat venom proteins possibly evade host immune response by the mutation of the surface chemistry through focal mutagenesis under the guidance of positive Darwinian selection. These results not only contribute to the body of knowledge regarding haematophagous venoms but also provide a rich resource for novel lead compounds for use in drug design and development.

Biological significance

These results have direct implications in understanding the molecular evolutionary history of vampire bat venom. The unusual peptides discovered reinforce the value of studying such neglected taxon for biodiscovery.

1. Introduction

Venom is defined as a secretion produced in a specialised gland in an animal, which is delivered to a target animal by inflicting a wound (regardless of size). Venom must also contain molecules (toxins) that disrupt normal physiological and/or biochemical processes so as to facilitate feeding or defence by the producing animal [1]. This definition includes secretions produced by blood feeding (haematophagous) specialists such as fleas, ticks, leeches or vampire bats that disrupt the haemostatic defences of prey/host organisms. These secretions which facilitate haematophagy or blood feeding are considered a particular subtype of venom.

With the level of infamy that extends far beyond the boundaries of science, blood-sucking vampire bats (Chiroptera, Desmodotinae) have been the subject of folk tales, superstitions and stories associated with the legendary Count Dracula for centuries [2,3]. All the three species of vampire bats are confined to Central and South America and typically live in the caves, tree hollows, and abandoned mines [4]. The relatively rare hairy-legged vampire bat (*Diphylla ecaudata*) feeds exclusively on avian hosts, while the white-winged vampire bat (*Diaemus youngi*) thrives on both the mammalian and avian blood, but most likely favouring the latter [2,5]. In contrast, the common vampire bat, *Desmodus rotundus* feeds overwhelmingly on mammals and has established itself in large colonies over an increasingly extensive distribution [2,6,7]. The expanding population of these bats is attributed to the increasing human population and the associated large number of domesticated animals and livestock, which provide a constant, high-density food supply [4,7].

All three species of vampire bats are highly specialised for a haematophagous lifestyle, especially *D. rotundus* [4]. Modifications of the teeth and limbs of vampire bats facilitate this lifestyle [6]. Reinforcement of limb strength permits *D. rotundus* and the other vampire bat species to approach their prey from the ground via quadrupedal walking and jumping [5,7,8]. *D. rotundus* is the most specialised of all vampire bats, and possesses specialised sensory capabilities for the detection of prey [9]. Close-range thermal and mechanical sensitivity is utilised for locating capillaries during feeding, while long-range vision, olfaction, acute hearing and echolocation are utilised for the discovery of potential prey [9]. They also have razor-like upper and lower incisors [5,7,10] that inflict a crater-shaped wound unique to *D. rotundus*. While feeding, their tongue darts in and out of the wound, releasing venom from the dorsal side of the tongue while drawing in blood via two straw-like ducts located on the ventral side of the tongue [7].

In order to facilitate blood-feeding, *D. rotundus* must be capable of interfering with their prey's natural haemostatic response to injury during feeding and digesting [11,12]. A typical haemostatic response produces a fibrin clot within minutes of the infliction of a wound, preventing further blood loss. The response commences with the constriction of blood vessels, restricting blood flow to the wound, and is followed by the adhesion of activated platelets to the site of injury and the conversion of fibrinogen to insoluble fibrin, forming a blood clot [12]. In contrast to this normal response to injury, bleeding from a wound induced by vampire bats may be prolonged from minutes to hours, ensuring a constant flow of blood for the bat to feed upon [12].

The gland predominantly associated with haematophagy in *D. rotundus* is the principle submaxillary gland, which consists of two separate anterior and posterior lobes [13]. This gland is responsible for the secretion of venom with strong anticoagulant and proteolytic activities [13]. The venom delays the onset of blood clotting by interfering with fibrin formation or acting upon fibrin as it is converted from fibrinogen. In addition it has a strong proteolytic action that breaks up any blood clots that may be formed. This proteolytic action is accomplished through the activation of the host's fibrinolytic system which converts plasminogen to plasmin, solubilising and removing fibrin clots to prevent excessive fibrin buildup at the site of the wound.

The venom of the vampire bat has been documented to disrupt the coagulation cascade via four distinct mechanisms: (i) inhibition of factor IXa, (ii) inhibition of factor Xa, (iii) activation of plasminogen and (iv) inhibition of platelets [1]. A venom component that has been researched considerably is draculin, an anticoagulant factor. It is an 88.5 kDa glycoprotein that inhibits activated factors IX (IXa) and X (Xa) of the coagulation mechanism [11,14,15]. The irreversibly bonded complex of Xa-Draculin forms immediately upon contact, inhibiting factors IXa and Xa [14]. The inhibition of IXa and Xa prevents the conversion of prothrombin to thrombin, which in turn prevents the conversion of fibrinogen to insoluble fibrin. Furthermore, the characteristic of non-competitive inhibition prevents the cleavage of draculin from Xa after binding, thus maintaining the toxin's anticoagulant activity during feeding and digestion [16]. Interestingly, a study conducted recently described the capacity of *D. rotundus* prey to develop immunity to draculin if they were targeted and fed upon over prolonged periods [17]. This kind of predator–prey arms race scenario is similar to that observed between other venomous animals and their prey.

The plasminogen activators or Desmokinase [12], better known as DSPA (*Desmodus rotundus* salivary plasminogen activator), are the most intensively researched vampire bat venom components and the only ones to have been characterised from all three species of vampire bats [12,18]. The non-venom form of plasminogen activator consists of five domains: fibronectin type-I; EGF-like; kringle 1 (K1); kringle 2 (K2); and serine protease. Plasminogen activators act upon fibrin clots, dissolving them and allowing a continuous flow of blood for feeding [12]. The ancestral vampire bat form, present in the avian feeding *D. ecaudata*, retains all these domains [18]. In contrast, the plasminogen activators isolated from the venom systems of the mammalian feeders all lack one or more domains. The generalist feeder *D. youngi* lacks the K2 domain as do all the isoforms found in the mammalian specialist *D. rotundus*. However, all four *D. rotundus* forms (DSPAα1, DSPAα2, DSPAβ and DSPAγ [19]) also lack the plasmin-sensitive activation site. In addition, DSPAβ and DSPAγ lack the fibronectin type-I domain. DSPAγ is the most derived form of this toxin in that it also lacks the EGF-like domain. Reflective of these domain variations, the two largest DSPA isoforms are DSPAα1 and α2, which share a 96% nucleotide sequence similarity (2165 out of 2245). The second largest DSPA is DSPAβ, which is composed of a 2107 nucleotide sequence (138 nucleotide deletions) and the smallest, DSPAγ, is composed of a 1996 nucleotide sequence (249 nucleotide deletions) [19,20].

The DSPAs, especially DSPAα1, are remarkably similar to the human tissue-type plasminogen activator (tPA), and have been extensively investigated for use as a thrombolytic drug for strokes [20]. Van Zonneveld et al. [21] established the importance of the finger (F) and kringle 2 (K2) domains for the binding of plasminogen activators to fibrin, both of which are present in tPA [19]. In spite of the K2 domain being absent in all four DSPA isoforms, they exhibit a kringle domain (K) that structurally resembles the kringle 1 (K1) domain in tPA, and functionally resembles tPA K2 domain [22]. The removal of the K2 domain not only facilitates increased specificity towards fibrin, it also decreases the plasminogen activator's susceptibility towards plasminogen activator inhibitor 1 (PAI-1), which is present in mammalian but absent in avian fibrin clots [23]. Despite having equivalent glycosylation sites as the endogenous form t-PA (tissue plasminogen activator), the vampire bat forms are differentially glycosylated, having more highly bioprocessed N-glycans than the high mannose counterpart in t-PA [24–26]. This difference results in the vampire bat forms being cleared at a four-fold lower rate than t-PA, resulting in a prolonged activity time. Another structural difference is that the lack of the plasmin-activation site also enables the *D. rotundus* forms, uniquely, to be potently active as single chains, rather than the t-PA which is fully active only as a two-chain form [18].

Despite the extensive research focused on the plasminogen activating activity of draculin and DSPA, investigation of other effects of the *D. rotundus* venom on the prey's hemostatic response has been limited. Hawkey [12] reported the presence of a vasodilator that triggered leakage of skin capillaries into surrounding tissues in guinea pigs, as well as the presence of platelet aggregation inhibitors that prevented the adhesion of platelets to foreign substances. As this manuscript was being prepared, a transcriptome study that overlapped with ours was published [27]. However, this study did not investigate the molecular evolution of the encoded venom proteins. Additionally, the different types of dominant transcripts between the studies are reflective of both variations in sequencing method and perhaps also regional/individual variations of study animals. For example, in this study we obtained draculin/lactotransferrin from the anterior and posterior lobes of the principal submaxillary gland while the other study recovered this protein type only from the accessory gland. Other types, such as calcitonin, were recovered from both glands through transcriptomics and proteomics in this study, but not discovered in the other study. In addition this study employed isoelectrically focused 2D gel analysis followed by LC–MS/MS guided mass spectrometry sequencing of in-gel digested spots as well as LC–MS/MS of trypsin digested crude secretions. Thus, the present study provides a much more in-depth investigation of the molecular evolution of secreted proteins, rather than providing a comprehensive catalogue which includes intracellular proteins as per [27].

2. Materials and methods

2.1. *Specimens*

Two adult male *D. rotundus* specimens were collected from Cuernavaca, Mexico by BGF and ACA using mist nets.

2.2. *Transcriptome library construction*

Anterior or posterior lobes of the principal submaxillary gland were dissected out and pooled and immediately frozen in liquid nitrogen for future use. Total RNA was extracted using the standard TRIzol Plus method (Invitrogen). Extracts were enriched for mRNA using standard RNeasy mRNA mini kit (Qiagen) protocol. mRNA was reverse transcribed, fragmented and ligated to a unique 10-base multiplex identifier (MID) tag prepared using standard protocols and applied to one PicoTitrePlate (PTP) for simultaneous amplification and sequencing on a Roche 454 GS FLX + Titanium platform (Australian Genome Research Facility). Automated grouping and analysis of sample-specific MID reads informatically separated sequences from the other transcriptomes on the plates, which were then post-processed to remove low quality sequences before de novo assembly into contiguous sequences (contigs) using v 3.4.0.1 of the MIRA software programme. Assembled contigs were processed using CLC Main Work Bench (CLC-Bio) and Blast2GO bioinformatic suite [28,29] to provide Gene Ontology, BLAST and domain/Interpro annotation. The above analyses assisted in the rationalisation of the large numbers of assembled contigs into phylogenetic 'groups' for detailed phylogenetic analyses outlined below that focused upon types detected in the proteome, rather than providing a comprehensive catalogue that included the various ordinary intracellular proteins (for such details, please see the parallel study [27]). Public access of the data can be found at the National Center for Biotechnology Information (NCBI) under bioproject PRJNA174817. Raw sequence reads can be downloaded from the short read archives (SRA) of the NCBI under number SRA061642. This Transcriptome Shotgun Assembly project has been deposited at DDBJ/EMBL/GenBank, under the accession GAEE00000000.

The version described in this paper, is the first version, GAEE01000000. Sequences are also directly available in Supplementary File 1.

2.3. Bioinformatics

2.3.1. Phylogenetics

Phylogenetic analyses were performed to allow reconstruction of the molecular evolutionary history of each toxin type for which transcripts were bioinformatically recovered. Toxin sequences were identified by comparison of the translated DNA sequences with previously characterised toxins using a BLAST search [30] of the UniProtKB protein database. Molecular phylogenetic analyses of toxin transcripts were conducted using the translated amino acid sequences. Comparative sequences from physiological gene homologs identified from non-venom gland transcriptomes were included in each dataset as outgroup sequences. To minimize confusion, all sequences obtained in this study are referred to by their GenBank accession numbers (http://www.ncbi.nlm.nih.gov/sites/entrez?db=Nucleotide) and sequences from previous studies are referred to by their UniProtKB accession numbers (http://www.expasy.org/cgi-bin/sprot-search-ful). Resultant sequence sets were aligned using CLC Mainbench. When presented as sequence alignments, the leader sequence is shown in lowercase and cysteines are highlighted in black. > and < indicate incomplete N/5′ or C/3′ ends, respectively. Datasets were analysed using the Bayesian inference implemented in MrBayes, version 3.0b4 [31], using lset rates=gamma with prset aamodelpr=mixed command to optimise between the nine amino acid substitution matrices implemented in MrBayes. The analysis was performed by running a minimum of 1×10^7 generations in four chains, and saving every 100th tree. The log-likelihood score of each saved tree was plotted against the number of generations to establish the point at which the log likelihood scores reached their asymptote, and the posterior probabilities for clades established by constructing a majority-rule consensus tree for all trees generated after completion of the burn-in phase.

2.3.2. Test for recombination

To overcome the effects of recombination on phylogenetic and evolutionary interpretations [32], we employed Single Breakpoint algorithms implemented in the HyPhy package and assessed recombination on all the toxin forms examined in this study [33,34]. When potential breakpoints were detected (depicted in Supplementary Figs. 1 and 2) using the small sample Akaike information Criterion (AICc), the sequences were compartmentalized before conducting the selection analyses.

2.3.3. Selection analyses

We evaluated selection pressures on *D. rotundus* venom components using maximum-likelihood models [35,36] implemented

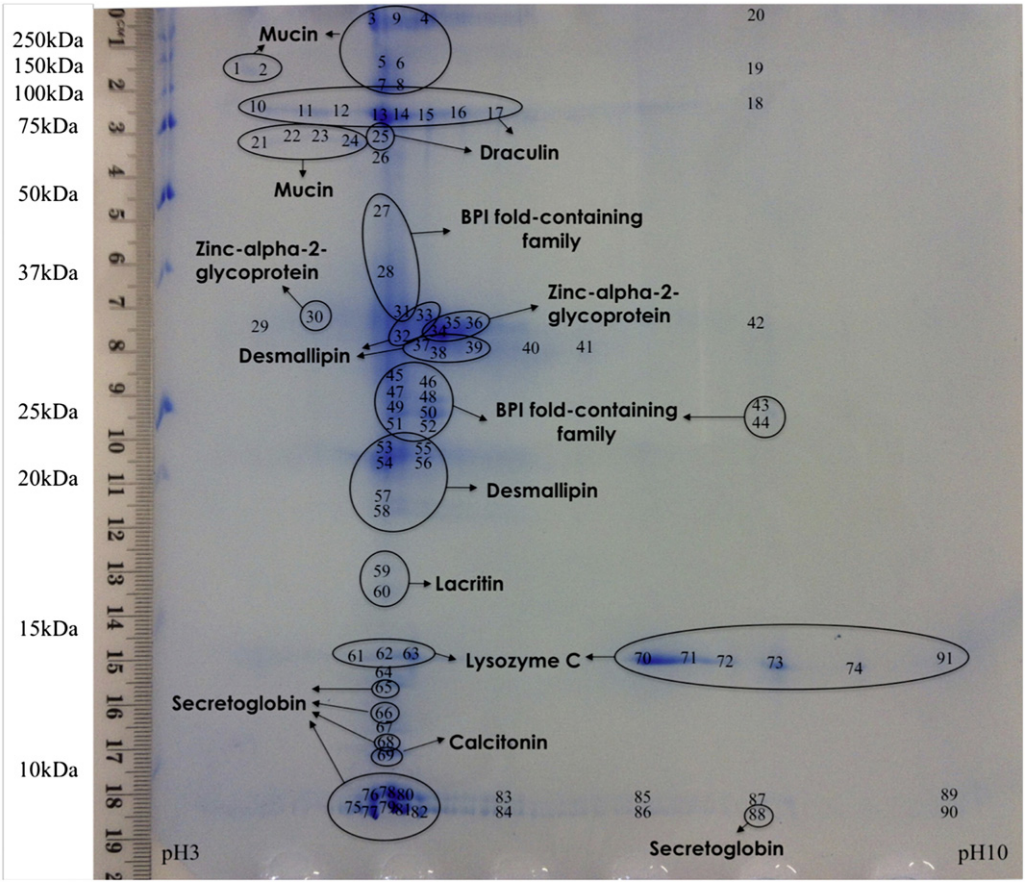

Fig. 1 – 2D gel electrophoresis of vampire bat venom.

Table 1 – Summary of *Desmodus rotundus* shotgun mass spectrometry sequencing.

Vampire bat (*Desmodus rotundus*) proteins	Matched peptides	% Total coverage
BPI-fold containing family	35	55
Calcitonin	13	21
Carbonic anhydrase 6	2	32
CRiSP (cysteine-rich secretory protein)	2	34
Desmallipin	60	43
Draculin	60	56
DSPA-alpha1	13	33
DSPA-beta	11	30
Glutathione peroxidase 3 (thioredoxin-like fold)	4	24
Haemoglobin-subunit beta	9	81
Igh protein	8	65
IGL@ protein	5	28
Immunoglobulin J chain	3	34
Kallikrein	10	68
Keratin	2	38
Kunitz-inhibitor	15	35
Lacritin	8	44
Desmallipin	5	45
Lysozyme C	5	23
Major urinary protein	3	37
Mucin	17	35
PACAP	9	10
Pancreatic secretory trypsin inhibitor (Kazal type)	2	22
Polymeric immunoglobulin receptor (immunoglobulin)	5	31
Proline-rich protein (Submaxillary gland androgen regulated protein)	2	26
Thrombospondin-1	18	34
Tumour necrosis factor (C-type lectin-like)	9	33
Secretoglobin	29	42
Semaphorin-3A (CD100 antigen)	1	40
Semaphorin-3A (immunoglobulin)	7	38
Statherin	1	11
Vasoactive intestinal peptide (glucagon-like)	2	13
WAP four-disulfide core domain protein (whey acidic protein)	2	42
Zinc-alpha-2-glycoprotein	10	46

Table 2 – Summary of *Desmodus rotundus* 2D gel spots and shotgun mass spectrometry.

Vampire bat (*Desmodus rotundus*) orthologous proteins	Spot number	Matched peptides	% Total overage
BPI fold-containing family	27, 28, 31, 43, 44, 45, 46, 47, 48, 49, 50, 51	45	32
Calcitonin	69	2	12
Desmallipin	32, 33, 37, 38, 39, 53, 54, 55, 56, 57, 58	50	36
Draculin	10, 11, 13, 14, 15, 16, 17, 25	63	44
Lacritin	59, 60	4	27
Lysozyme C	61, 63, 70, 71, 72, 73, 74, 91	38	38
Mucin	1, 3, 5, 6, 7, 8, 9, 21, 22, 24	22	12
Secretoglobin	65, 66, 68, 75, 76, 77, 79, 80, 81, 82, 88	32	42
Zinc-alpha-2-glycoprotein	30, 34, 35, 36	18	31

in CODEML of the PAML [37]. We first employed the one-ratio model that assumes a single ω for the entire phylogenetic tree. This model tends to be very conservative and can only detect positive selection if the ω ratio averaged over all the sites along the lineage is significantly greater than one. Because such lineage-specific models assume a single ω for the entire tree, they often fail to identify regions in proteins that might be affected by episodic selection pressures and ultimately, underestimate the strength of selection. Hence, we employed site-specific models which estimate positive selection statistically as a non-synonymous-to-synonymous nucleotide-substitution rate ratio (ω) significantly greater than 1. We compared likelihood values for three pairs of models with different assumed ω distributions as no a priori expectation exists for the same: M0 (constant ω rates across all sites) versus M3 (allows the ω to vary across sites within 'n' discrete categories, $n \geq 3$); M1a (a model of neutral evolution) where all sites are assumed to be either under negative ($\omega < 1$) or neutral selection ($\omega = 1$) versus M2a (a model of positive selection) which in addition to the site classes mentioned for M1a, assumes a third category of sites; sites with $\omega > 1$ (positive selection) and M7 (Beta) versus M8 (Beta and ω), and models that mirror the evolutionary constraints of M1 and M2 but assume that ω values are drawn from a beta distribution [38]. Only if the alternative models (M3, M2a and M8: allow sites with $\omega > 1$) show a better fit in Likelihood Ratio Test (LRT) relative to their null models (M0, M1a and M8: do not show allow sites $\omega > 1$), are their results considered significant. LRT is estimated as twice the difference in maximum likelihood values between nested models and compared with the χ^2 distribution with the appropriate degree of freedom — the difference in the number of parameters between the two models. The Bayes empirical Bayes (BEB) approach [39] was used to identify amino acids under positive selection by calculating the posterior probabilities that a particular amino acid belongs to a given selection class (neutral, conserved or highly variable). Sites with greater posterior probability (PP ≥ 95%) of belonging to the 'ω > 1 class' were inferred to be positively selected.

Fast, Unconstrained Bayesian AppRoximation (FUBAR) implemented in HyPhy [40] was employed to provide additional support to codeml analyses and to detect sites evolving under the influence of pervasive diversifying and purifying selection pressures. Mixed Effects Model Evolution (MEME) [41] was also used to detect episodic diversifying selection. Further support for the results of the selection analyses was obtained using a complementary amino acid-level approach implemented in TreeSAAP [42]. We assessed selection pressures shaping multi-domain proteins by employing the option

Table 3 – Activities of homologues to *Desmodus rotundus* venom proteins.

Protein type	Activity of related proteins
BPI-fold	Generalised property of this class is antimicrobial [60].
Calcitonin	Generalised property of this class is vasodilation [61].
CRiSP	Shown in snake venoms to be neurotoxic [62–65]
Draculin	Demonstrated effect in vampire bat venom is anticoagulation through inhibition of FIXa and FXa [11,12,15,16].
Desmallipin	Salivary androgen-binding protein [66]
DSPA	Demonstrated effect in vampire bat venom plasminogen activation [18]
Kallikrein	Vasodilation and cleavage of fibrinogen [67]
Kunitz	Forms in other venoms are anticoagulant in various ways such as inhibition of FVIIa, FXa or thrombin [68–72]
Lacritin	Promotes secretion [73]
Lysozyme	Antibacterial [74]
Mucin	Saliva lubrication [75]
PACAP-related/PACAP/novel-peptide tripeptide precursor	Vampire bat forms untested but related to PACAP peptides are vasodilatory [76]. Bioactivity of any PACAP-related peptide is unknown.
Secretoglobin	Anti-inflammatory or immunomodulatory properties [77]
Stathlipin	-Unknown-
Waprin	Antimicrobial [78]
Zinc-alpha-2-glycoprotein	Lipid degradation [79]

G test (with Mgene = 4) [43]. We further employed branch-site REL [44] to identify lineages undergoing episodic adaptations.

2.3.4. *Structural analyses*

In order to depict the selection pressures influencing the evolution of *D. rotundus* venom components, we mapped the sites under positive selection on the homology models created using Phyre 2 webserver [45]. Pymol 1.3 [46] was used to visualize and generate the images of homology models. Consurf webserver [47] was used for mapping the evolutionary selection pressures on the three-dimensional homology models. GETAREA [48] was used to calculate the Accessible Surface Area (ASA) or the solvent exposure of amino acid side chains. It uses the atom coordinates of the PDB file and indicates if a residue is buried or exposed to the surrounding medium by comparing the ratio between side-chain Accessible Surface Area (ASA) and the "random coil" values per residue. An amino acid is considered to be buried if it has an ASA less than 20% and exposed if ASA is more than or equal to 50%. An ASA ratio between 40% and 50% indicates partial exposure of amino acid side chains.

2.3.5. *Proteomics*

Specimens were anaesthetized using zoletil (3 mg/kg) and then injected subcutaneously with pilocarpine (20 mg/kg) to stimulate salivation. Polyethylene equipment was used to collect and process samples in all cases. Samples were subsequently filtered using 20 Å syringe filters to remove large mucoidal strands and then lyophilised.

For two-dimensional electrophoresis, venom samples (~2 mg) were directly solubilised in 300 μl of rehydration buffer (8 M urea, 100 mM DTT, 4% CHAPS, 110 mM DTT, and 0.5% ampholytes (Biolytes pH 3–10)) and 0.01% bromophenol blue. Sample was mixed and centrifuged (5 min, 4 °C, 14,000 rpm) to pellet any insoluble material and the supernatant was loaded onto IEF strips (Bio-Rad ReadyStrip, non-linear pH 3–10, 17 cm IPG) for 24 h passive rehydration. Proteins were focused in a PROTEAN i12 IEF CELL (Bio-Rad Lab, USA). The IEF running conditions were as follows: 100 V for 1 h, 500 V for 1 h 1000 V for 1 h and 8000 V for 98,400 V/h. After running IEF, IPG strips were equilibrated for 10 min in an equilibration buffer (50 mM Tris–HCl, pH 8.8, 6 M urea, 2% SDS, 30% glycerol, 2% DTT) followed by a second incubation for 20 min in an equilibration buffer that had DTT replaced with 2.5% iodoacetamide. IPG strips were briefly rinsed in SDS-PAGE running buffer and embedded on top of the 12% polyacrylamide gels (Protean-II Plus, 18 × 20 cm, Bio-Rad Lab, USA) and covered with 0.5% agarose. Second dimension gels were performed at 4 °C for 10 mA/per gel for 20 min followed by 30 mA/per gel for 4 h or until the bromophenol dye front was reached to 1 cm from the base of the gel. Finally gels were briefly wash in Milli-Q water and stain in 0.2% colloidal Coomassie brilliant blue G250 (34% methanol, 3% phosphoric acid, 170 g/l ammonium sulphate, 1 g/l Coomassie blue G250) overnight and destained in 1% acetic acid/H_2O. Visible spots were subsequently picked from gels and digested overnight (at 37 °C) using sequencing grade trypsin (Sigma, USA). Briefly, gel spots were washed with ultrapure water, destained (40 mM NH_4CO_3/50% Acetonitrile (ACN)) and dehydrated (100% ACN). Gel spots were rehydrated in 10 μl of 20 μg/ml proteomic grade trypsin (Sigma-Aldrich) and incubated at 37 °C overnight. Digests were eluted by washing the gel spots for 20 min with each of the following solutions: 20 μl 1% formic acid (FA), followed by 20 μl of 5% ACN/0.5% FA. The cleaved peptides were eluted and thereafter subjected to LC–MS/MS analysis.

For shotgun sequencing, reduction and alkylation was performed by redissolving 3 μg of sample in 50 μl of 100 mM ammonium carbonate. 50 μl of 2% iodoethanol/0.5% triethylphosphine in acetonitrile was then added to the re-dissolved samples. The reduced and alkylated sample was re-suspended in 20 μl of 40 mM ammonium bicarbonate, before being incubated overnight (at 37 °C) with 750 ng proteomic grade trypsin. Digestion was stopped by addition of 1 μl of concentrated formic acid. 0.75 μg was processed by LC–MS/MS.

LC–MS/MS was done using a Agilent Zorbax stable bond C18 column (2.1 mm × 100 mm, 1.8 μm particle size, 300 Å pore size) at a flow of 400 μl/min and a gradient of 1–40%

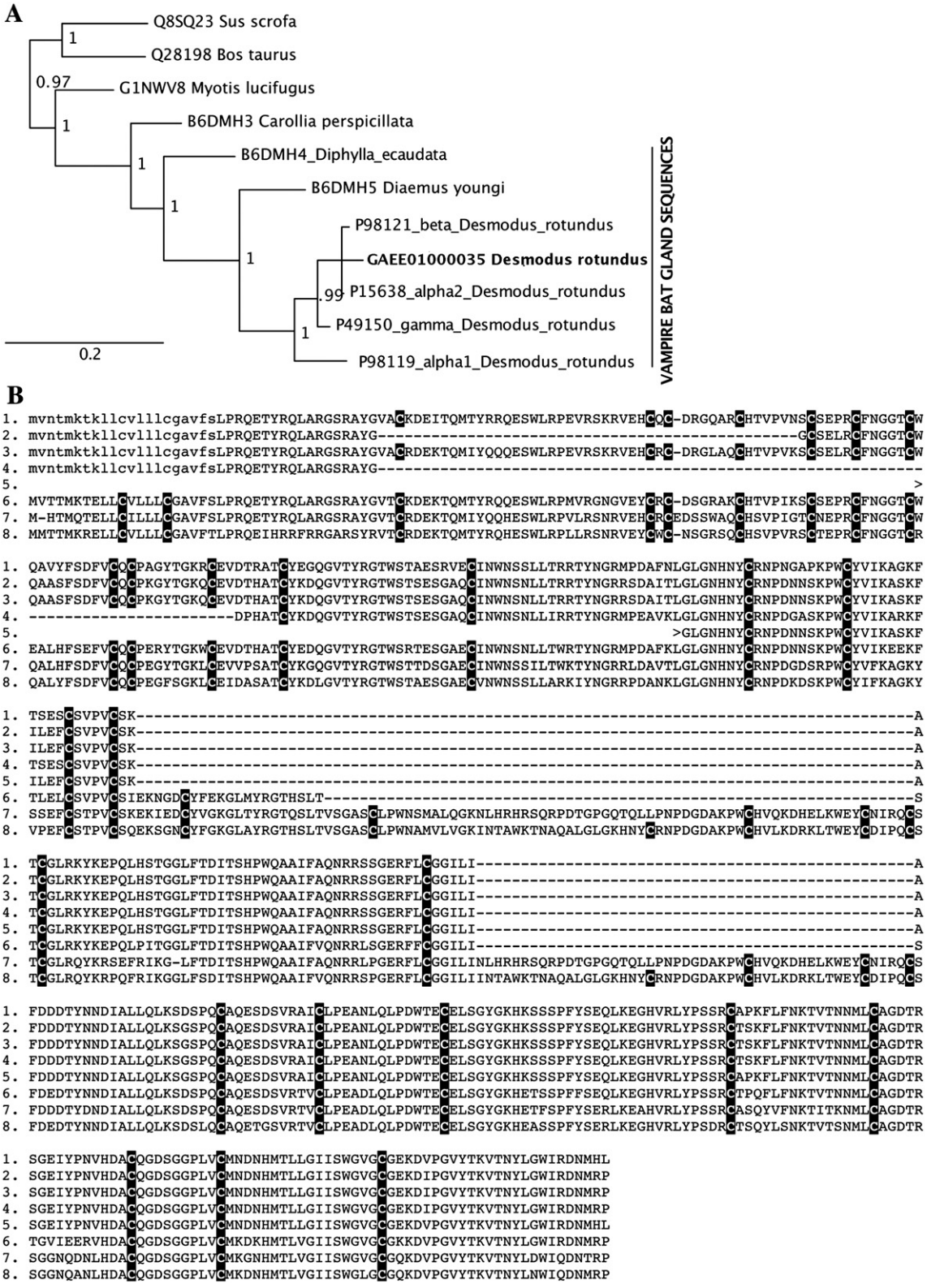

Fig. 2 – A) Precursor phylogenetic reconstruction. B) Sequence alignment of vampire bat venom plasminogen activator precursors from *Desmodus rotundus* venom (1. DSPA-5 (GAEE01000035) in this study and the previously sequenced (and also obtained in this study) 2. P49150 (gamma DSPA), 3. P98121 (beta DSPA), 4. P98119 (alpha1 DSPA), 5. P15638 (alpha2 DSPA)), *Diaemus youngi* (6. B6DMH5), *Diphylla ecaudata* (7. B6DMH4) and the non-venom, normal blood version from the bat *Myotis lucifugus* (8. G1NWV8).

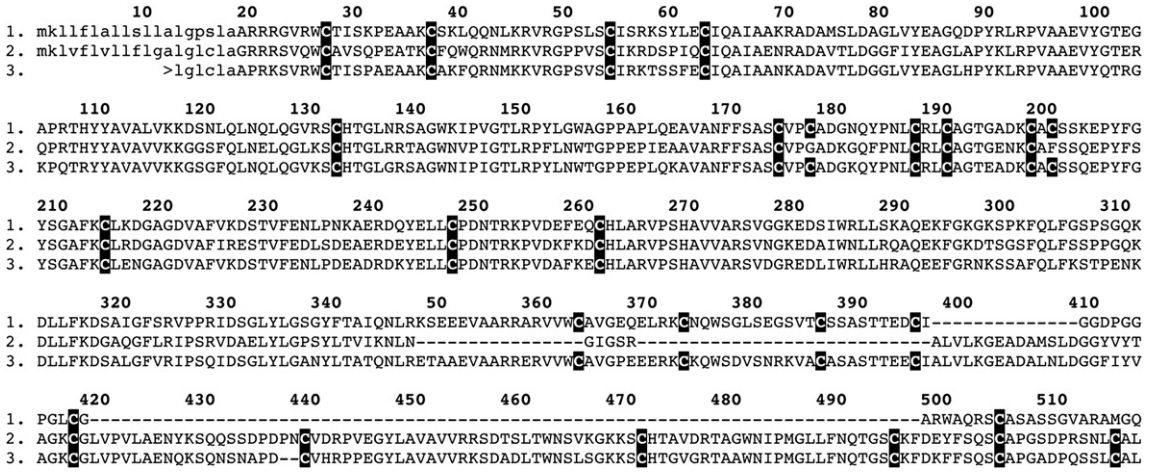

Fig. 3 – Alignment of the precursors 1. Draculin-1 (GAEE01000036) with non-venom lactotransferrin from 2. *Homo sapiens* (P02788) and 3. *Equus caballus* (O77811).

solvent B (90% acetonitrile, 0.1% formic acid) in 0.1% formic acid over 15 min or 4 min for shotgun and 2D-gel spots, respectively, on a Shimadzu Nexera UHPLC coupled with an AB SCIEX 5600 Triple TOF mass spectrometer. MS^2 spectra were acquired at a rate of 20 scans/s, with a cycle time of 2.3 s, and optimised for high resolution. Precursor ions were selected between 80 and 1800 m/z, charge state of 2–5, and of an intensity of at least 120 counts per second, with a precursor selection window of 1.5 Da, and excluding isotopes within 2 Da for MS^2. MS^2 spectra were searched against known translated cDNA libraries or UniProt databanks with ProteinPilot v4.0 (ABSciex) using a thorough identification search, specifying alkylation method (iodoacetamide or iodoethanol), tryptic digestion, and allowing for biological and chemical modifications and amino acid substitution. This was done to maximize the identification of protein sequences from the transcriptome despite the inherent variability of toxins, and potential isoform mismatch with the transcriptomic data. Spectra were inspected manually to eliminate false positives, and the results further analysed using CLC Main Workbench v6.6. Full search conditions are shown in Supplementary File 2.

3. Results

3.1. *Proteomics and transcriptomics*

Through our combined proteomic and transcriptomic approach, with the proteomic results guiding the selection of transcripts to focus on for molecular evolutionary investigations, we discovered a rich suite of secreted proteins in *D. rotundus* venom glands (Fig. 1, Tables 1, 2 and 3; Supplementary Tables 1 and 2). The same peptide/protein types sequenced in the transcriptomes were also detected in the proteome, demonstrating concordance between transcription and translation. DSPA isoforms were difficult to detect in the 2D gel due to the high levels of glycosylation interfering with efficient colloidal staining but DSPA α1, α2, β and γ isoforms were readily detected in the shotgun sequencing, reflective of its significant level of secretion. We also recovered a partial sequence (with overlapping fragments from both lobes) that was unique in being sequentially and phylogenetically intermediate between the alpha2 and beta forms of DSPA (Fig. 2). The partial sequence did not contain the region where alpha2 and beta differ in domain loss, so relative affinity could not be fully ascertained. Until recently [27], draculin had long only been known from a small 16 amino acid fragment and it was thus unknown which protein family the toxin belonged to. In this study, we recovered a 1164 base-pair partial sequence (incomplete on the 3′ end) that revealed draculin to be a member of the lactotransferrin family secreted in the submaxillary glands (Fig. 3).

We also recovered and identified protein types previously unknown from vampire bat venom, or sequenced in the concurrent parallel study [27], with related non-venomous isoforms having characterised activities including anticoagulation (Kunitz peptides), immunomodulation (BPI fold-containing family A, secretoglobin), secretion promotion (lacritin), peripheral vasodilation (CRiSP) and vasodilation (calcitonin, kallikrein and PACAP). We further identified a highly modified version of the salivary androgen-binding protein/allergen-protein family that included the major cat allergen fel-d4 and the major horse allergen Equ-c1, and also an extremely derived form of the statherin peptide type (Table 1). Transcriptome analysis revealed Kunitz and PACAP to be multi-domain precursors. Kunitz peptides were derived from an ancestral tri-product encoding precursor, with the basal form expressed in the submaxillary gland being bi-domain (Fig. 4). Additional derived forms include loss of the first or second domains of the bi-domain form. The PACAP peptides were also encoded by a bi-domain precursor, that includes not only the vasodilatory PACAP peptide, but also the PACAP-related peptide, the activity of which remains undiscovered (Fig. 5A). Both domains preserved the high alpha-helical content of the ancestral non-venom peptides (Fig. 5B). The newly derived vampire bat form had two distinct isoform types that formed a discrete clade within the ancestral peptide family

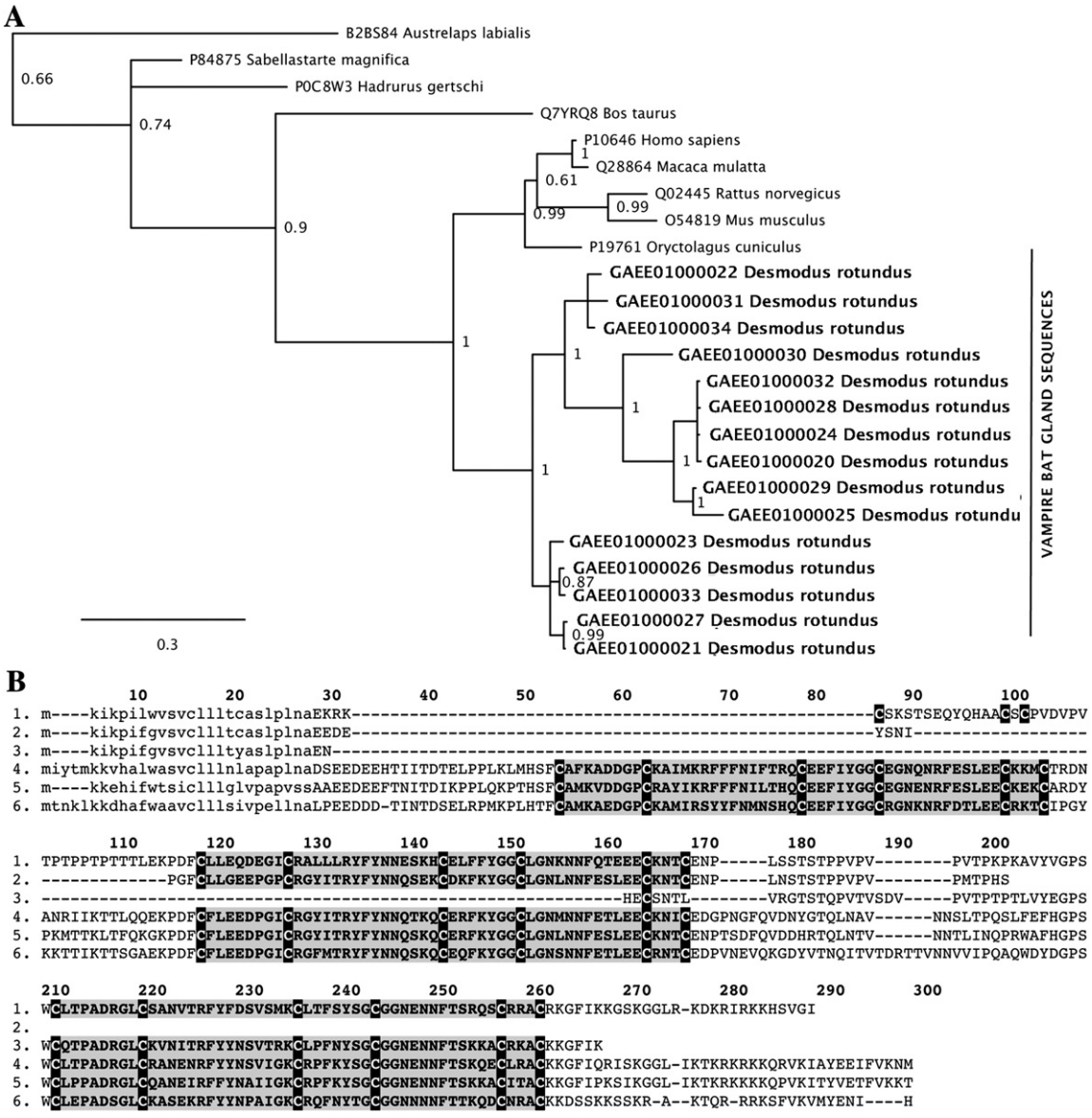

Fig. 4 – A) Precursor phylogenetic reconstruction. B) Sequence alignment of Kunitz peptide precursors from *Desmodus rotundus* venom. 1. Representative dual domain form Dro-kunitz-1 (GAEE01000020), representatives of the mono-domain variants (2. Dro-kunitz-4 (GAEE01000023) and 3. Dro-kunitz-5 (GAEE01000024)) and the non-venom forms from 4. *Homo sapiens* (P10646), 5. *Oryctolagus cuniculus* (P19761) and 6. *Rattus norvegicus* (Q02445).

(Fig. 5C). In addition, our proteomic studies revealed that a third peptide is post-translationally cleaved from within this precursor (Fig. 5A). This peptide is located upstream from the other two peptides and starts at the point where the signal peptide is cleaved off, and is characterised by being proline rich. The allergen-related lipocalin proteins (which we termed Desmallipins as an acronym for 'desmodus allergen-related lipocalins') contained an N-terminal region cysteine not present in the ancestral form from the bat *Myotis lucifugus* (Fig. 6). Some of the submaxillary gland forms had an additional newly-evolved cysteine located between the first and second ancestral cysteines. While the calcitonin peptides were highly conserved relative to the ancestral peptides (Fig. 7) the statherin-peptide type (stathlipin) differed considerably from the ancestral form in the number and pattern of C-terminal region prolines (Fig. 8).

3.2. *Molecular evolution*

The global omega values computed using the one-ratio model (ORM) for different *D. rotundus* venom components ranged from indicating positive selection (Desmallipins: ω =1.03; Plasminogen Activator: ω = 1.04) to near-neutral evolution (PACAP: ω = 0.86) and negative selection (Kunitz domain I: ω =0.29; Kunitz domain II: ω = 0.39) (Supplementary Tables 3.1–3.5). Since ORM averages dN/dS over the entire length of the coding sequence, it often fails to detect episodic diversifying selection that is confined to small regions of protein. Hence, we employed the site-specific models (Table 4; Figs. 9 and 10; Supplementary Table 3.1–3.5). Site-model 8 highlighted the dominant role of positive selection on the evolution of *D. rotundus* venom components: Desmallipins ω = 1.28; Kunitz domain I ω = 1.39;

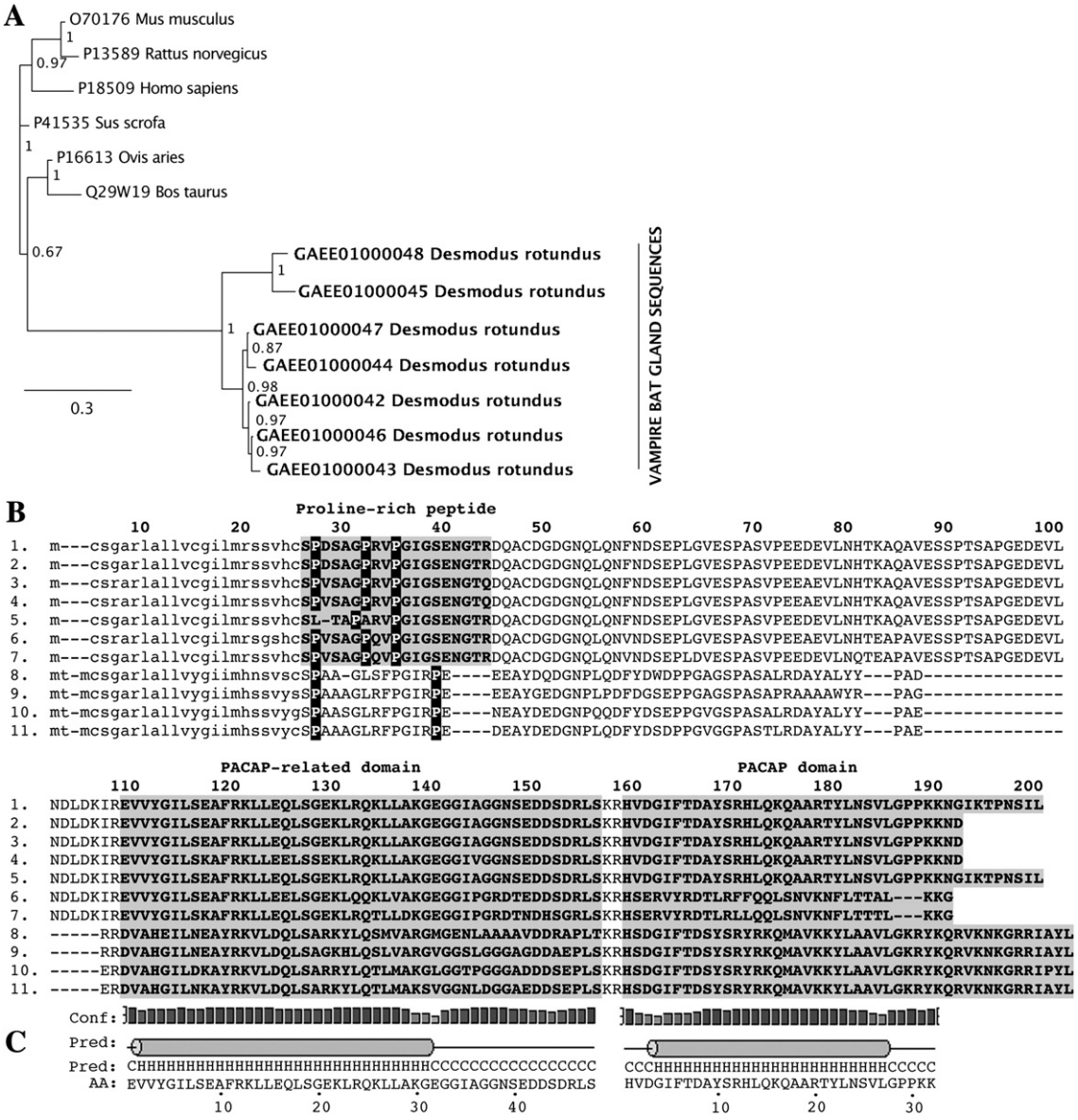

Fig. 5 – PACAP A) Precursor phylogenetic reconstruction, B) sequence alignment of PACAP-precursors from *Desmodus rotundus* venom (1. PACAP3-Dr-5, 2. PACAP3-Dr-1, 3. PACAP3-Dr-6, 4. PACAP3-Dr-3, 5. PACAP3-Dr-2, 6. PACAP3-Dr-7, 7. PACAP3-Dr-4) and the non-venom forms from 8. *Rattus norvegicus* (P13589), 9. *Homo sapiens* (P18509), 10. *Ovis aries* (P16613), 11. *Sus scrofa* (P41535). Post-translationally cleaved peptides are high-lighted in grey. C) Alpha-helical content of a representative vampire bat peptide is shown under the alignment.

Kunitz domain II ω = 1.28; PACAP ω = 1.24 and plasminogen activator ω = 1.23. The BEB approach implemented in site-model 8 detected large proportions of sites in aforementioned toxins as evolving under the influence of positive selection: Desmallipins [22% and 18 positively selected sites (PS)]; Kunitz domain I (28% and 4 PS); Kunitz domain II (35% and 5 PS); PACAP (20% and 7 PS) and plasminogen activator (36% and 23 PS) (Table 4 and Supplementary Tables 3.1–3.5).

We further employed option G test to compare the evolutionary regimes adopted by different PACAP and plasminogen activator domains. This test computed differential evolutionary rates for various PACAP domains. The propeptide domain was extremely conserved and evolved under the regime of negative selection (ω = 0.43). Extremely low amount of non-synonymous to synonymous mutations detected in this region suggests that it is likely involved in efficient excision and liberation of PACAP domains (Fig. 10). This test further revealed that both PACAP-related (ω = 1.75) and PACAP (ω = 1.59) domains evolve rapidly under the influence of positive selection (Fig. 10). Option G test also highlights the differential evolution of *D. rotundus* plasminogen activator domains (Fibronectin type-I: ω = 0.86; EGF-like: ω = 0.90 and Kringle domain: ω = 1.08 and peptidase-s1 ω = 0.91) (Fig. 10).

Not all non-synonymous mutations are capable of influencing a change in the structure and/or function of the protein. This is especially true when the mutant amino acid has the identical or similar biochemical properties as its ancestral amino acid. Such mutations are more likely to have no effect on the fitness

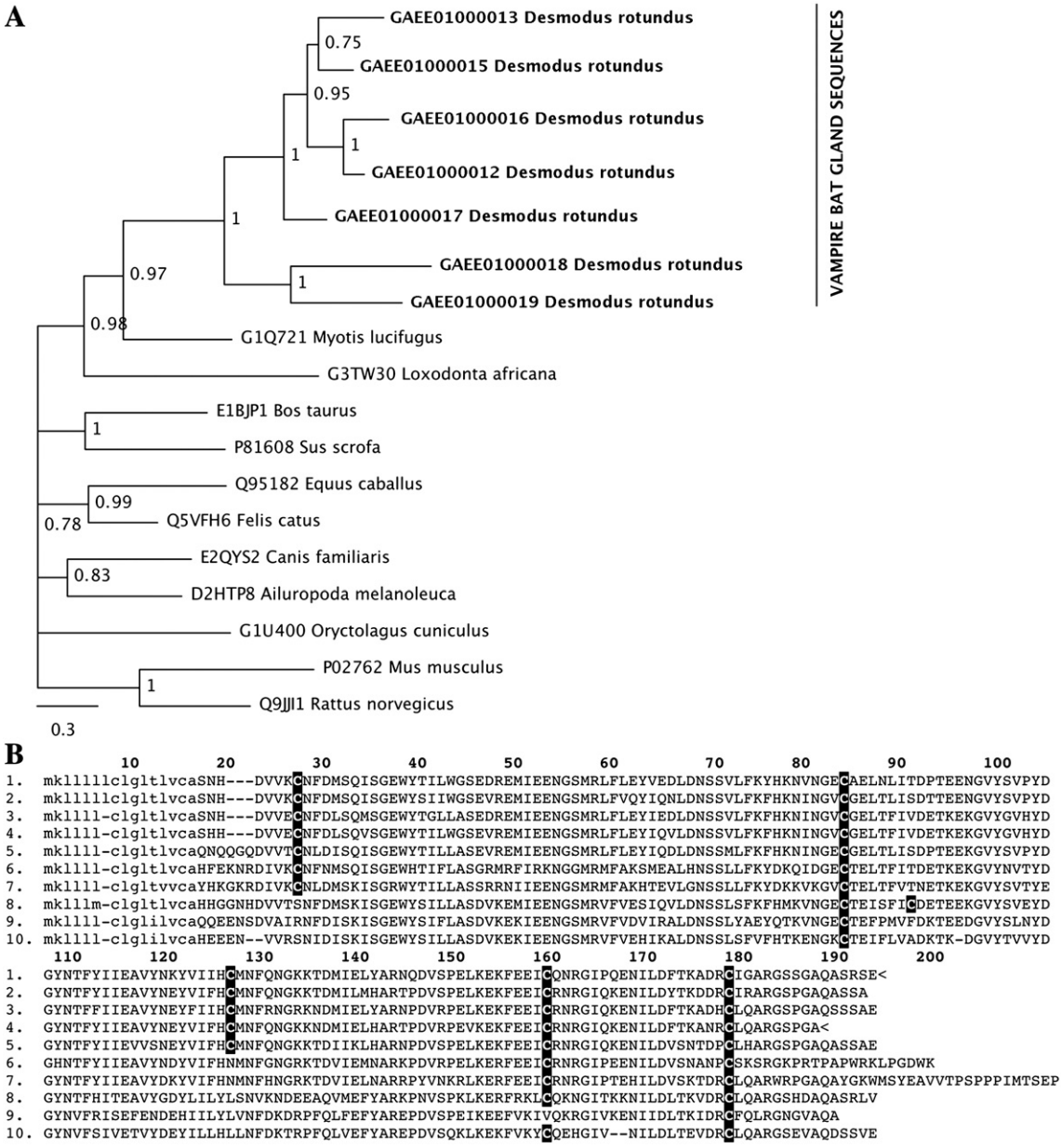

Fig. 6 – A) Precursor phylogenetic reconstruction. B) Sequence alignment of equ-c1/fel-d4 related precursors from *Desmodus rotundus* venom (1. Desmallipin-2 (GAEE01000013), 2. Desmallipin-4 (GAEE01000015), 3. Desmallipin-5 (GAEE01000016), 4. Desmallipin-1 (GAEE01000012), 5. Desmallipin-6 (GAEE01000017), 6. Desmallipin-7 (GAEE01000018), 7. Desmallipin-8 (GAEE01000019)), and the non-venom forms from 8. *Myotis lucifugus* (G1Q721), 9. *Equus caballus* (Q95182), and 10. *Felis catus* (Q5VFH6).

of the organism. In order to decide which mutations could have a greater impact on the structure and/or function of the protein, we assessed the selective influence on 31 structural and biochemical amino acid properties using TreeSAAP (Supplementary Table 4). TreeSAAP measures the selective influences during cladogenesis, and performs goodness-of-fit and categorical statistical tests based on ancestral sequence reconstruction. This combined approach revealed that Desmallipins, Kunitz (domain I and II) and plasminogen activator genes accumulated radical mutations which introduced amino acids with quite divergent biochemical and/or structural properties (Supplementary Table 4). On the contrary, none of the positively selected sites detected by PAML in PACAP were identified as positively selected by the protein-level analyses. Hence, we theorize that the rapid radical changes accumulating in Desmallipins (83% positively selected sites), Kunitz (89% positively selected sites) and plasminogen activators (48% positively selected sites) are more likely to have a greater impact on the fitness of these vampire bats than the hypermutable sites of PACAP proteins (Supplementary Table 4). Evolutionary fingerprint of vampire bat toxins revealed a large proportion of sites as evolving under the significant influence of positive selection (Supplementary Fig. 3). Branch-site REL test (Supplementary Fig. 4) identified several branches in all

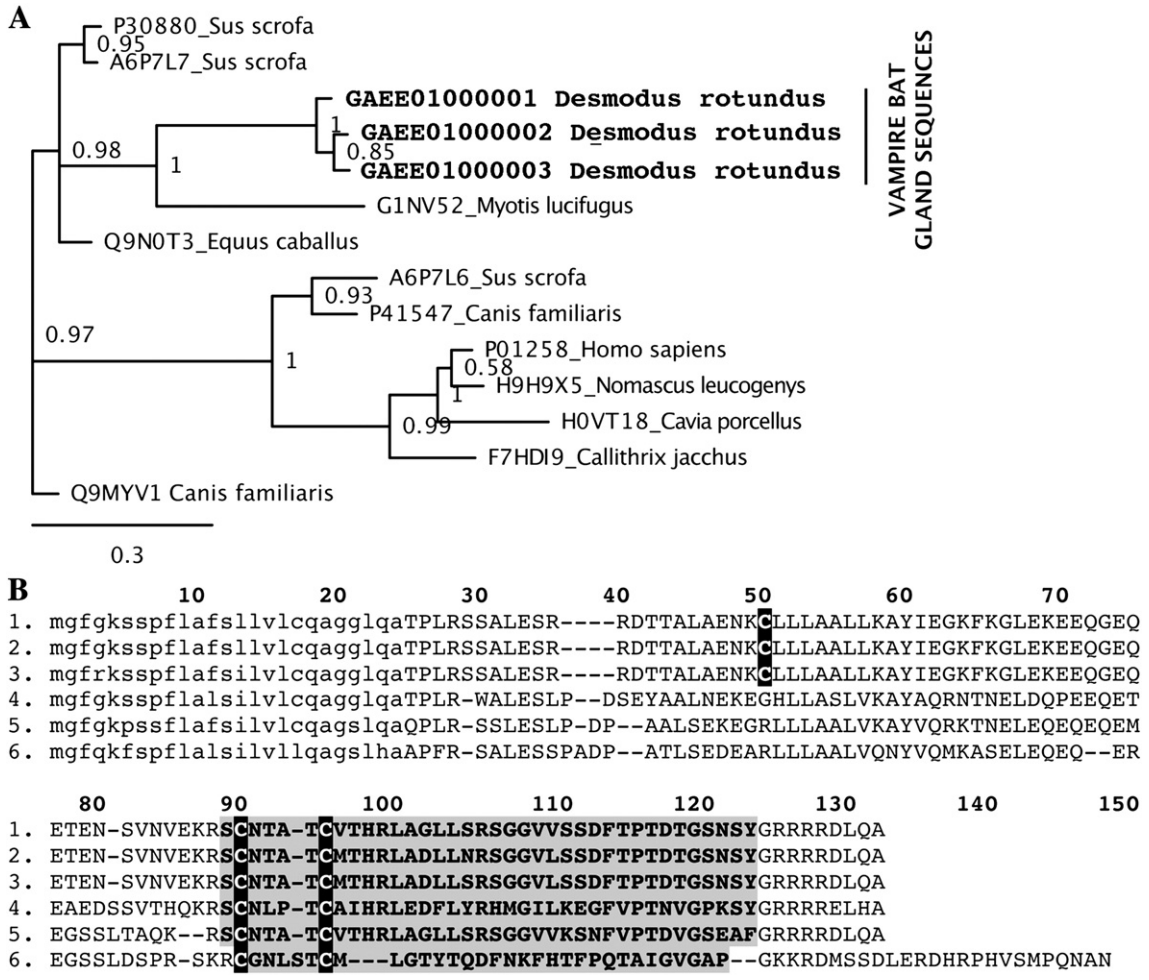

Fig. 7 – A) Calcitonin precursor phylogenetic reconstruction. B) Sequence alignment of calcitonin peptide precursors from *Desmodus rotundus* venom (1. calcitonin-Dro-1 (GAEE01000001), 2. calcitonin-Dro-2 (GAEE01000002), 3. calcitonin-Dro-3 (GAEE01000001) and the non-venom forms from, 4. *Myotis lucifugus* (G1NV52), 5. *Equus caballus* (Q9N0T3), and 6. *Homo sapiens* (P01258)). Post-translationally cleaved peptides are shown in grey.

the vampire bat toxin lineages examined in this study as episodically diversifying: Desmallipins (7), PACAP (4), Kunitz (9) and plasminogen activator (2).

Thus, evidence provided by various selection analyses [site-specific model 2a, 3, 8; FUBAR, MEME; protein-level analyses: (Table 4; Figs. 9 and 10; Supplementary Tables 3.1–3.5 and 4), Evolutionary fingerprint analyses (Supplementary Fig. 3), Branch-site REL (Supplementary Fig. 4) and option G test] suggested a strong influence of positive selection on *D. rotundus* venom components examined in this study.

4. Discussion

It was previously unclear whether the principal gland anterior and posterior lobes were evolving on different evolutionary trajectories, or if they remained under shared genetic control. Recovery of identical transcripts from the cDNA libraries in this study provides evidence that they remain a single expression system. Multiple transcripts of the majority of each protein type were recovered from the cDNA libraries,

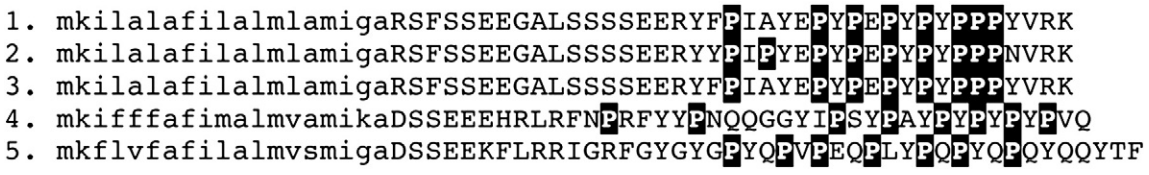

Fig. 8 – Sequence alignment of stalipin peptide precursors from *Desmodus rotundus* (Stalipin-Dr-1 (GAEE01000051), Stalipin-Dr-2 (GAEE01000052), Stalipin-Dr-3 (GAEE01000053)) and the related non-venom peptides from *Bos taurus* (Q8HY86) and *Homo sapiens* (P02808).

Table 4 – Molecular evolution of *Desmodus rotundus* (vampire bat) venom-components.

Toxin type	FUBAR[a]		PAML			MEME sites[b]
Desmallipins				M8	M2a	9
	$\omega > 1$[c]	14	$\omega > 1$[e]	18	13	
	$\omega < 1$[d]	6		(12 + 6)	(6 + 7)	
	$\omega =$	–	$\omega =$	1.28	1.27	
Kunitz (overall)	$\omega > 1$[g]	9	$\omega > 1$[e]	16	17	7
	$\omega < 1$[h]	34		(6 + 10)	(6 + 11)	
	$\omega =$	–	$\omega =$	1.45	1.67	
Kunitz domain I	$\omega > 1$[g]	0	$\omega > 1$[e]	4	0	1
	$\omega < 1$[h]	8		(2 + 2)		
	$\omega =$	–	$\omega =$	1.39	0.55^{NS}	
Kunitz domain II	$\omega > 1$[g]	3	$\omega > 1$[e]	5	1	1
	$\omega < 1$[h]	15		(1 + 4)	(0 + 1)	
	$\omega =$	–	$\omega =$	1.28	1.21	
PACAP	$\omega > 1$[g]	4	$\omega > 1$[e]	7	2	3
	$\omega < 1$[h]	4		(1 + 6)	(1 + 4)	
	$\omega =$	–	$\omega =$	1.24	1.24	
Plasminogen activator	$\omega > 1$[g]	16	$\omega > 1$[e]	23	17	1
	$\omega < 1$[h]	3		(6 + 17)	(2 + 15)	
	$\omega =$	–	$\omega =$	1.23	1.27	
Calcitonin	Not enough sequences for analyses (n = 3). All three sequences were extremely conserved.					

PACAP: Pituitary Adenylate Cyclase-Activating Polypeptide; Desmallipins: Desmodus allergen-related lipocalins
Legend:
a: Fast Unbiased Approximate Bayesian.
b: Sites detected as experiencing episodic diversifying selection (0.05 significance) by the Mixed Effects Model Evolution (MEME).
c: Number of sites detected by FUBAR as under pervasive diversifying selection at the posterior probability ≥ 0.9.
d: Number of sites detected by FUBAR as under pervasive purifying selection at the posterior probability ≥ 0.9.
e: Number of positively selected sites detected using the Bayes Empirical Bayes approach implemented in M8 and M2a. Sites detected at 0.99 and 0.95 significance are indicated in the parenthesis.
ω: mean dN/dS.
NS: Not significant.

a pattern consistent with accelerated diversification in toxin multigene families as observed in other venoms [49–51]. The differential domain loss in the Kunitz peptide followed a pattern of selection pressure for the expression of particularly useful domains, such as seen in reptile venoms ([52,53] and Fig. 10). Numerous transcripts were recovered with significant variations including changes in key functional residues and changes in the number of cysteine residues, modifications typically associated with neofunctionalisation (evolution of novel bioactivities).

Cysteine number variation was particularly evident in the Desmallipins, which are extremely intriguing as they represent a convergent modification of the fel-d4/equ-c1 type allergen scaffold, derived forms of which have been documented as the primary protein toxin in the venom of *Nycticebus* sp. (slow lorises) [54]. The ancestral proteins formed cysteine-linked homodimers, thus any modification of cysteine-pattern may greatly affect the structure of the monomer and thus its ability to form dimers. In the basal form of *D. rotundus* Desmallipins, there is an even number of cysteines, and thus these isoforms may not form dimers at all, but rather monomers with a unique structural fold. In the further derived forms, there is another new cysteine, which may promote dimerisation but with a unique three-dimensional structure of each subunit. Our identification of draculin as a lactotransferrin with a neofunctionalised activity is further proof of the principle that vampire bats are modifying ancestral molecular scaffolds for new targeting.

Another form of neofunctionalisation seen in other venoms is guided not through variations in cysteine pattern, but rather through changes in relative proline-bracketing of linear peptides, such as seen in the helokinestatin peptides [53,55]. Such de novo creation of a new post-translationally liberated proline-rich domain was seen in the third PACAP-precursor peptide discovered in this study. While the sthalipin peptides evolved from the proline-rich statherin peptides, significant changes in the number and pattern was evident.

Nucleotide and complementary amino acid-level selection analyses (Supplementary Table 4) provide the first evidence that *D. rotundus* venom components evolve under the regime of positive selection, accumulating rapid mutations. However, not all mutations seem to have a significant impact on the structure and function of these toxins; only the mutations in Kunitz (domain I and II), Desmallipins and plasminogen activators were identified by protein-level selection assessments as capable of introducing radical changes. Hence, we theorize that mutations in these toxins are not only capable of affecting the structure and function of the toxin, but may also influence the fitness of vampire bats (Supplementary Table 4).

All the positively selected sites in *D. rotundus* Kunitz (domain I and domain II) and 43% of positively selected sites in plasminogen activator (22% buried; rest couldn't be conclusively assigned to exposed/buried class) were found on the molecular surface of the toxin (Supplementary Table 4). A strong evolutionary constraint on the non-secreted PACAP propeptide, reflective of its role in efficient liberation of toxin

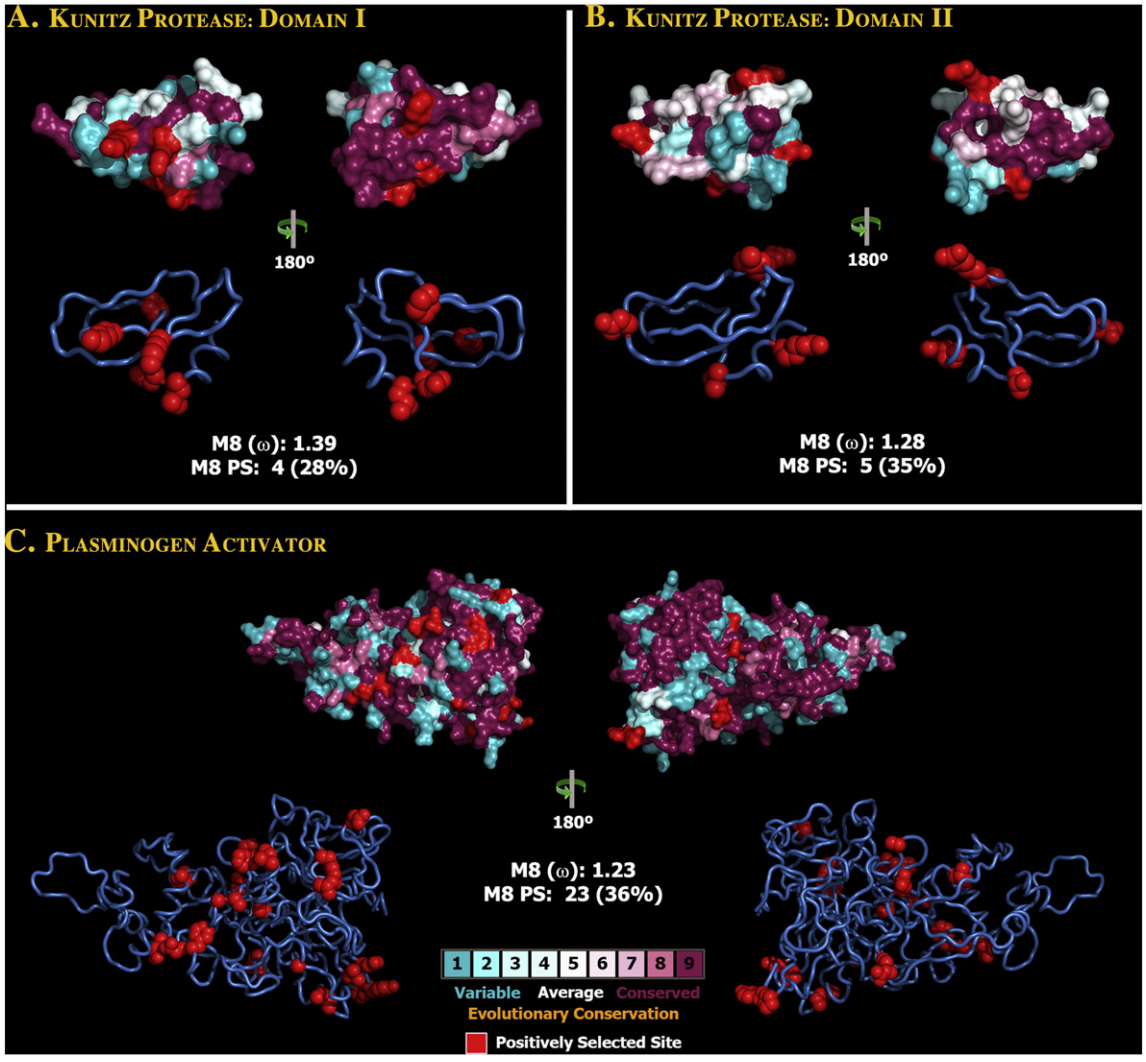

Fig. 9 – A, B and C: Three-dimensional homology models of *D. rotundus* venom components depicting the locations of positively selected sites in red (M8, PP ≥ 0.95, Bayes-Empirical Bayes approach) and relative conservation of surface residues on a scale of 1–9 (1: most variable; 9: most conserved) are presented. Site-model 8 computed omega value and the number of positively (PS) sites (percentage of sites indicated in parenthesis) detected by its Bayes Empirical Bayes approach are also presented.

domains, and on the active sites of plasminogen activator gene was observed (Fig. 10 and Supplementary Fig. 1). We theorize that focal mutagenesis, in which a large proportion of mutations are confined to the molecular surface (Supplementary Table 4) and structurally and/or functionally unimportant regions (Supplementary Figs. 1 and 2), not only aids in conservation of structural and functional integrity of these toxins, but may also prevent the mounting of immunological resistance against these secretions in prey animals. Evidently, prey animals of *D. rotundus* have been shown to develop immunity to venom components like draculin if targeted and fed upon over prolonged periods [17]. Hence, we hypothesize that frequent mutation of toxin molecular surface chemistry in vampire bat population prevents the rapid development of immunological resistance in prey–animals. Focal or site-directed mutagenesis has been demonstrated in a wide array of venom proteins, as a means of preserving residues responsible for structural and/or functional stability, while generating rapid variation of the molecular surface of venom [56–59]. Thus, toxins in a diversity of venomous lineages have likely, convergently adopted site-directed mutagenesis or focal mutagenesis as a strategy to evade immune responses of their prey animals.

5. Conclusion

The recovery of novel protein scaffolds from the glands studied here reveals how little is known about the protein composition of vampire bat venoms. This is further reinforced by the number and diversity of novel scaffolds recovered, despite the relatively limited sampling employed. More extensive sampling will no doubt recover entirely new toxin classes. Follow-up investigations should focus on the structure–function relationships of the novel components. These results highlight the relatively untapped potential of such complex mixtures as sources of

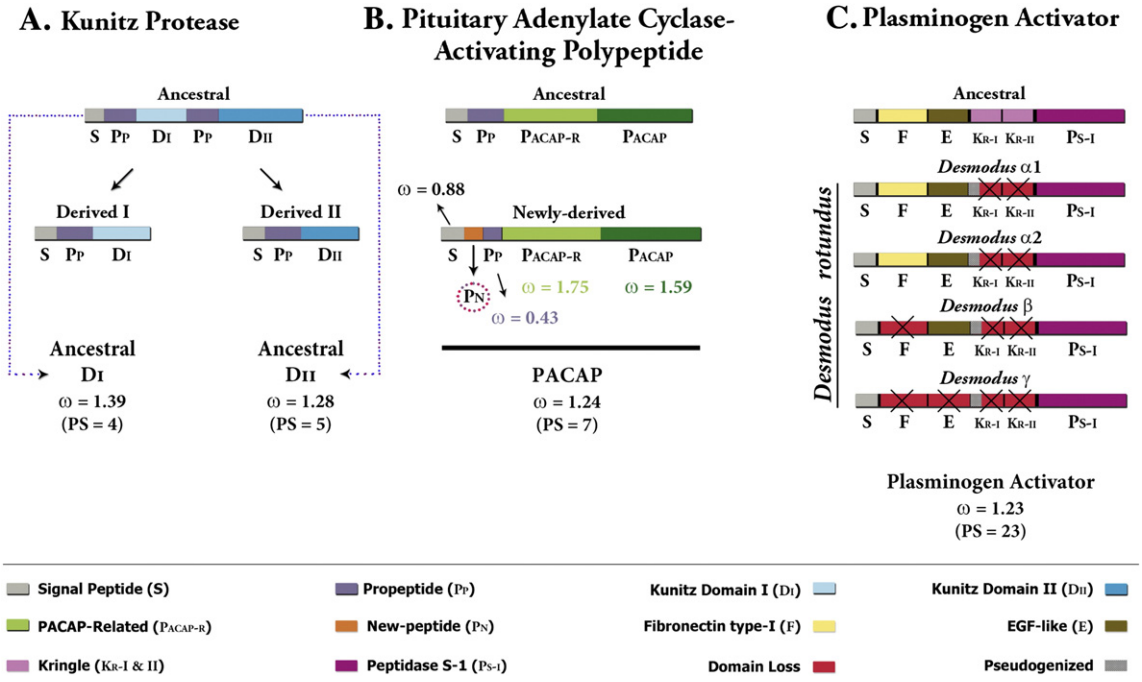

Fig. 10 – A, B, and C depict the molecular evolution of various *D. rotundus* toxin domains. A. Kunitz peptides are expressed as bi-domain (ancestral) and two types of derived mono-domain forms. B. Pituitary Adenylate Cyclase-Activating Polypeptide is expressed with a new-peptide carved out of the ancestral prepro domain. C. *D. rotundus* salivary secretion consists of four plasminogen activator isoforms (α1, α2, β, γ), all of which have lost one or more ancestral domains. Site-model 8 computed omega value and the number of positively (PS) sites detected by its Bayes Empirical Bayes approach are also presented.

novel investigation ligands or lead compounds for use in drug design and development. It is hoped that these results will stimulate further investigation of the hitherto neglected venom systems of all species of vampire bat.

Supplementary data to this article can be found online at http://dx.doi.org/10.1016/j.jprot.2013.05.034.

Acknowledgements

BGF was funded by the Australian Research Council and the University of Queenland. SAA was a recipient of postdoctoral fellowship (PDRF Phase II Batch-V) from the Higher Education Commission (HEC Islamabad) Pakistan. KS was funded by a PhD grant (SFRH/BD/61959/2009) from F.C.T. (Fundação para a Ciência e a Tecnologia). AA was funded by the project PTDC/AACAMB/121301/2010 (FCOMP-01-0124-FEDER-019490) from F.C.T. EABU would like to acknowledge funding from the University of Queensland (International Postgraduate Research Scholarship, UQ Centennial Scholarship, and UQ Advantage Top-Up Scholarship) and the Norwegian State Education Loans Fund.

REFERENCES

[1] Fry BG, Roelants K, Champagne DE, Scheib H, Tyndall JD, King GF, et al. The toxicogenomic multiverse: convergent recruitment of proteins into animal venoms. Annu Rev Genomics Hum Genet 2009;10:483–511.

[2] Tuttle MD. In: Greenhall AM, Schmidt U, editors. Introduction to the natural history of vampire bats. United States: CRC Press; 1988. p. 1–6.

[3] Villa CB, Canela RM. Man, gods, and legendary vampire bats. In: Greenhall AM, Schmidt U, editors. Natural history of vampire bats. United States: CRC Press; 1988. p. 233–40.

[4] Ray CE, Linares OJ, Morgan GS. Paleontology.United States: CRC Press; 1988 (Natural hi:19–30).

[5] Koopman KF. Systematics and distribution. In: Greenhall AM, Schmidt U, editors. Natural history of vampire bats. CRC Press; 1988. p. 7–18.

[6] Bhatnagar KP. Systematics and distribution. In: Greenhall AM, Schmidt U, editors. Natural history of vampire bats. CRC Press; 1988. p. 41–70.

[7] Greenhall AM. Feeding behavior. In: Greenhall AM, Schmidt U, editors. Natural history of vampire bats. CRC Press; 1988. p. 111–32.

[8] Altenbach JS. Natural history of vampire bats. Locomotion; 1988 71–84.

[9] Schmidt U. Systematics and distribution. In: Greenhall AM, Schmidt U, editors. Natural history of vampire bats. CRC Press; 1988. p. 143–66.

[10] Hawkey C. Inhibitor of platelet aggregation present in saliva of the vampire bat *Desmodus rotundus*. Br J Haematol 1967;13:1014–20.

[11] Basanova AV, Baskova IP, Zavalova LL. Vascular-platelet and plasma hemostasis regulators from bloodsucking animals. Biochem Biokhim 2002;67:143–50.

[12] Hawkey CM. Salivary antihemostatic factorsIn: Gree, editor. ; 1988. p. 133–42.

[13] Disanto PE. Anatomy and histochemistry of the salivary glands of the vampire bat, *Desmodus rotundus murinus*. J Morphol 1960;106:301–35.

[14] Fernandez AZ, Tablante A, Beguin S, Hemker HC, Apitz-Castro R. Draculin, the anticoagulant factor in vampire bat saliva, is a tight-binding, noncompetitive inhibitor of activated factor X. Biochim Biophys Acta 1999;1434:135–42.
[15] Apitz-Castro R, Beguin S, Tablante A, Bartoli F, Holt JC, Hemker HC. Purification and partial characterization of draculin, the anticoagulant factor present in the saliva of vampire bats (*Desmodus rotundus*). Thromb Haemost 1995;73: 94–100.
[16] Fernandez AZ, Tablante A, Bartoli F, Beguin S, Hemker HC, Apitz-Castro R. Expression of biological activity of draculin, the anticoagulant factor from vampire bat saliva, is strictly dependent on the appropriate glycosylation of the native molecule. Biochim Biophys Acta 1998;1425:291–9.
[17] Delpietro HA, Russo RG. Acquired resistance to saliva anticoagulants by prey previously fed upon by vampire bats (*Desmodus rotundus*): evidence for immune response. J Mamm 2009;90:1132–8.
[18] Tellgren-Roth A, Dittmar K, Massey SE, Kemi C, Tellgren-Roth C, Savolainen P, et al. Keeping the blood flowing-plasminogen activator genes and feeding behavior in vampire bats. Naturwissenschaften 2009;96:39–47.
[19] Kratzschmar J, Haendler B, Langer G, Boidol W, Bringmann P, Alagon A, et al. The plasminogen activator family from the salivary gland of the vampire bat *Desmodus rotundus*: cloning and expression. Gene 1991;105:229–37.
[20] Gulba DC, Praus M, Witt W. DSPA alpha — properties of the plasminogen activators of the vampire bat *Desmodus rotundus*. Fibrinolysis 1995;9:91–6.
[21] Van Zonneveld AJ, Veerman H, Pannekoek H. On the interaction of the finger and the kringle-2 domain of tissue-type plasminogen activator with fibrin. Inhibition of kringle-2 binding to fibrin by epsilon-amino caproic acid. J Biol Chem 1986;261:14214–8.
[22] Gardell SJ, Duong LT, Diehl RE, York JD, Hare TR, Register RB, et al. Isolation, characterization, and cDNA cloning of a vampire bat salivary plasminogen activator. J Biol Chem 1989;264:17947–52.
[23] Dellas C, Loskutoff DJ. Historical analysis of PAI-1 from its discovery to its potential role in cell motility and disease. Thromb Haemost 2005;93:631–40.
[24] Gohlke M, Nuck R, Kannicht C, Grunow D, Baude G, Donner P, et al. Analysis of site-specific N-glycosylation of recombinant *Desmodus rotundus* salivary plasminogen activator rDSPA alpha 1 expressed in Chinese hamster ovary cells. Glycobiology 1997;7:67–77.
[25] Gohlke M, Baude G, Nuck R, Grunow D, Kannicht C, Bringmann P, et al. O-linked L-fucose is present in *Desmodus rotundus* salivary plasminogen activator. J Biol Chem 1996;271:7381–6.
[26] Ligabue-Braun R, Verli H, Carlini CR. Venomous mammals: a review. Toxicon 2012;59:680–95.
[27] Francischetti IMB, Assumpção TCF, Ma D, Li Y, Vicente EC, Uieda W, et al. The "vampirome": transcriptome and proteome analysis of the principal and accessory submaxillary glands of the vampire bat *Desmodus rotundus*, a vector of human rabies. J Proteomics 2013;82:288–319.
[28] Gotz S, Garcia-Gomez JM, Terol J, Williams TD, Nagaraj SH, Nueda MJ, et al. High-throughput functional annotation and data mining with the Blast2GO suite. Nucleic Acids Res 2008;36:3420–35.
[29] Gotz S, Arnold R, Sebastian-Leon P, Martin-Rodriguez S, Tischler P, Jehl MA, et al. B2G-FAR, a species-centered GO annotation repository. Bioinformatics 2011;27:919–24.
[30] Altschul SF, Madden TL, Schaffer AA, Zhang J, Zhang Z, Miller W, et al. Gapped BLAST and PSI-BLAST: a new generation of protein database search programs. Nucleic Acids Res 1997;25: 3389–402.
[31] Ronquist F, Teslenko M, Van der Mark P, Ayres DL, Darling A, Hohna S, et al. MrBayes 3.2: efficient Bayesian phylogenetic inference and model choice across a large model space. Syst Biol 2012;61:539–42.
[32] Posada D, Crandall KA. The effect of recombination on the accuracy of phylogeny estimation. J Mol Evol 2002;54:396–402.
[33] Kosakovsky Pond SL, Posada D, Gravenor MB, Woelk CH, Frost SDW, Pond SLK. Automated phylogenetic detection of recombination using a genetic algorithm. Mol Biol Evol 2006;23: 1891–901.
[34] Delport W, Poon AF, Frost SD, Kosakovsky Pond SL. Datamonkey 2010: a suite of phylogenetic analysis tools for evolutionary biology. Bioinformatics 2010;26:2455–7.
[35] Goldman N, Yang Z. A codon-based model of nucleotide substitution for protein-coding DNA sequences. Mol Biol Evol 1994;11:725–36.
[36] Yang Z. Likelihood ratio tests for detecting positive selection and application to primate lysozyme evolution. Mol Biol Evol 1998;15:568–73.
[37] Yang Z. PAML 4: phylogenetic analysis by maximum likelihood. Mol Biol Evol 2007;24:1586–91.
[38] Nielsen R, Yang Z. Likelihood models for detecting positively selected amino acid sites and applications to the HIV-1 envelope gene. Genetics 1998;148:929–36.
[39] Yang Z, Wong WSW, Nielsen R. Bayes empirical Bayes inference of amino acid sites under positive selection. Mol Biol Evol 2005;22:1107–18.
[40] Murrell B, Moola S, Mabona A, Weighill T, Sheward D, Kosakovsky Pond SL, et al. FUBAR: a Fast, Unconstrained Bayesian AppRoximation for inferring selection. Mol Biol Evol 2013;30(5):1196–205.
[41] Murrell B, Wertheim JO, Moola S, Weighill T, Scheffler K, Kosakovsky Pond SL. Detecting individual sites subject to episodic diversifying selection. PLoS Genet 2012;8: e1002764.
[42] Woolley S, Johnson J, Smith MJ, Crandall KA, McClellan DA. TreeSAAP: selection on amino acid properties using phylogenetic trees. Bioinformatics 2003;19:671–2.
[43] Yang Z. Maximum-likelihood models for combined analyses of multiple sequence data. J Mol Evol 1996;42:587–96.
[44] Kosakovsky Pond SL, Murrell B, Fourment M, Frost SDW, Delport W, Scheffler K, et al. A random effects branch-site model for detecting episodic diversifying selection. Mol Biol Evol 2011;28:3033–43.
[45] Kelley LA, Sternberg MJ. Protein structure prediction on the Web: a case study using the Phyre server. Nat Protoc 2009;4: 363–71.
[46] DeLano WL. The PyMOL molecular graphics system. San Carlos, CA: DeLano Scientific; 2002 .
[47] Armon A, Graur D, Ben-Tal N. ConSurf: an algorithmic tool for the identification of functional regions in proteins by surface mapping of phylogenetic information. J Mol Biol 2001;307: 447–63.
[48] Fraczkiewicz R, Braun W. Exact and efficient analytical calculation of the accessible surface areas and their gradients for macromolecules. J Comput Chem 1998;19:319–33.
[49] Duda TF, Palumbi SR. Molecular genetics of ecological diversification: duplication and rapid evolution of toxin genes of the venomous gastropod Conus. Proc Natl Acad Sci U S A 1999;96:6820–3.
[50] Fry BG. From genome to "venome": molecular origin and evolution of the snake venom proteome inferred from phylogenetic analysis of toxin sequences and related body proteins. Genome Res 2005;15:403–20.
[51] Fry BG, Wüster W, Kini RM, Brusic V, Khan A, Venkataraman D, et al. Molecular evolution and phylogeny of elapid snake venom three-finger toxins. J Mol Evol 2003;57:110–29.
[52] Fry BG, Wüster W. Assembling an arsenal: origin and evolution of the snake venom proteome inferred from

phylogenetic analysis of toxin sequences. Mol Biol Evol 2004;21:870–83.
[53] Fry BG, Roelants K, Winter K, Hodgson WC, Griesman L, Kwok HF, et al. Novel venom proteins produced by differential domain-expression strategies in beaded lizards and gila monsters (genus *Heloderma*). Mol Biol Evol 2010;27:395–407.
[54] Hagey LR, Fry BG, Fitch-Snyder H. Talking defensively: a dual use for the brachial gland exudate of slow and pygmy lorises; 2006 289–308.
[55] Fry BG, Winter K, Norman JA, Roelants K, Nabuurs RJ, Van Osch MJP, et al. Functional and structural diversification of the Anguimorpha lizard venom system. Mol Cell Proteomics 2010;9:2369–90.
[56] Sunagar K, Johnson WE, O'Brien SJ, Vasconcelos V, Antunes A. Evolution of CRISPs associated with toxicoferan-reptilian venom and mammalian reproduction. Mol Biol Evol 2012;29:1807–22.
[57] Brust A, Sunagar K, Undheim EB, Vetter I, Yang DC, Casewell NR, et al. Differential evolution and neofunctionalization of snake venom metalloprotease domains. Mol Cell Proteomics 2013;12:651–63.
[58] Ruder T, Sunagar K, Undheim EEB, Ali S, Wai T-C, Low DW, et al. Molecular phylogeny and evolution of the proteins encoded by coleoid (cuttlefish, octopus, and squid) posterior venom glands. J Mol Evol 2013:1–13.
[59] Kini RM, Chan YM. Accelerated evolution and molecular surface of venom phospholipase A2 enzymes. J Mol Evol 1999;48:125–32.
[60] Labro MT. Interference of antibacterial agents with phagocyte functions: immunomodulation or "immuno-fairy tales"? Clin Microbiol Rev 2000;13:615–50.
[61] Smillie SJ, Brain SD. Calcitonin gene-related peptide (CGRP) and its role in hypertension. Neuropeptides 2011;45:93–104.
[62] Yamazaki Y, Brown RL, Morita T. Purification and cloning of toxins from elapid venoms that target cyclic nucleotide-gated ion channels. Biochemistry 2002;41:11331–7.
[63] Yamazaki Y, Morita T. Structure and function of snake venom cysteine-rich secretory proteins. Toxicon 2004;44:227–31.
[64] Yamazaki Y, Koike H, Sugiyama Y, Motoyoshi K, Wada T, Hishinuma S, et al. Cloning and characterization of novel snake venom proteins that block smooth muscle contraction. Eur J Biochem 2002;269:2708–15.
[65] Yamazaki Y, Hyodo F, Morita T. Wide distribution of cysteine-rich secretory proteins in snake venoms: isolation and cloning of novel snake venom cysteine-rich secretory proteins. Arch Biochem Biophys 2003;412:133–41.
[66] Karn RC, Laukaitis CM. Characterization of two forms of mouse salivary androgen-binding protein (ABP): implications for evolutionary relationships and ligand-binding function. Biochemistry 2003;42:7162–70.
[67] Hofmann W, Junk A, Geiger R. Human tissue kallikrein. II. Isolation and characterization of human salivary kallikrein. Hoppe Seylers Z Physiol Chem 1983;364(4):425–32.
[68] Campbell CL, Wilson WC, Manninen K. Characterization of differentially expressed midge genes in *Orbivirus* vector populations. Am J Trop Med Hyg 2005;73:144.
[69] Campbell CL, Vandyke KA, Letchworth GJ, Drolet BS, Hanekamp T, Wilson WC. Midgut and salivary gland transcriptomes of the arbovirus vector *Culicoides sonorensis* (Diptera: Ceratopogonidae). Insect Mol Biol 2005;14:121–36.
[70] Li S, Kwon J, Aksoy S. Characterization of genes expressed in the salivary glands of the tsetse fly, *Glossina morsitans morsitans*. Insect Mol Biol 2001;10:69–76.
[71] Francischetti IM, Andersen JF, Ribeiro JM. Biochemical and functional characterization of recombinant *Rhodnius prolixus* platelet aggregation inhibitor 1 as a novel lipocalin with high affinity for adenosine diphosphate and other adenine nucleotides. Biochemistry 2002;41:3810–8.
[72] Francischetti IM, Valenzuela JG, Andersen JF, Mather TN, Ribeiro JM. Ixolaris, a novel recombinant tissue factor pathway inhibitor (TFPI) from the salivary gland of the tick, *Ixodes scapularis*: identification of factor X and factor Xa as scaffolds for the inhibition of factor VIIa/tissue factor complex. Blood 2002;99:3602–12.
[73] Sanghi S, Kumar R, Lumsden A, Dickinson D, Klepeis V, Trinkaus-Randall V, et al. cDNA and genomic cloning of lacritin, a novel secretion enhancing factor from the human lacrimal gland. J Mol Biol 2001;310:127–39.
[74] Fabian TK, Hermann P, Beck A, Fejerdy P, Fabian G. Salivary defense proteins: their network and role in innate and acquired oral immunity. Int J Mol Sci 2012;13:4295–320.
[75] Zalewska A, Zwierz K, Zółkowski K, Gindzieński A. Structure and biosynthesis of human salivary mucins. Acta Biochim Pol 2000;47:1067–79.
[76] Vaudry D, Falluel-Morel A, Bourgault S, Basille M, Burel D, Wurtz O, et al. Pituitary adenylate cyclase-activating polypeptide and its receptors: 20 years after the discovery. Pharmacol Rev 2009;61:283–357.
[77] Mukherjee AB, Cordella-Miele E, Kikukawa T, Miele L. Modulation of cellular response to antigens by uteroglobin and transglutaminase. Adv Exp Med Biol 1988;231:135–52.
[78] Hagiwara K, Kikuchi T, Endo Y, Huqun X, Usui K, Takahashi M, et al. Mouse SWAM1 and SWAM2 are antibacterial proteins composed of a single whey acidic protein motif. J Immunol 2003;170:1973–9.
[79] Russell ST, Zimmerman TP, Domin BA, Tisdale MJ. Induction of lipolysis in vitro and loss of body fat in vivo by zinc-alpha2-glycoprotein. Biochim Biophys Acta 2004;1636(1):59–68.